Supporting Information

Hydrazine Hydrate Intercalated 1T-dominant MoS_2 with Superior Ambient Stability for Highly Efficient Electrocatalytic Applications

Mengyao Li[a], Zizhen Zhou[a], Long Hu[b], Shuangyue Wang[a], Yingze Zhou[a], Renbo Zhu[a], Xueze Chu[c], Ajayan Vinu[c], Tao Wan[a,], Claudio Cazorla[d,]*, Jiabao Yi[c,]*, and Dewei Chu[a]*

[a] School of Materials Science and Engineering, University of New South Wales, Sydney, NSW 2052, Australia

E-mail: tao.wan@unsw.edu.au

[b] School of Engineering, Macquarie University Sustainable Energy Research Centre, Macquarie University, Sydney, NSW, 2109 Australia

[c] Global Innovative Centre for Advanced Nanomaterials, College of Engineering, Science and Environment, The University of Newcastle, Callaghan, NSW 2308, Australia

E-mail: jiabao.yi@newcastle.edu.au

[d] Department de Física, University Politècnica de Catalunya, Campus Nord B4-B5, 08034, Barcelona, Spain

E-mail: claudio.cazorla@upc.edu

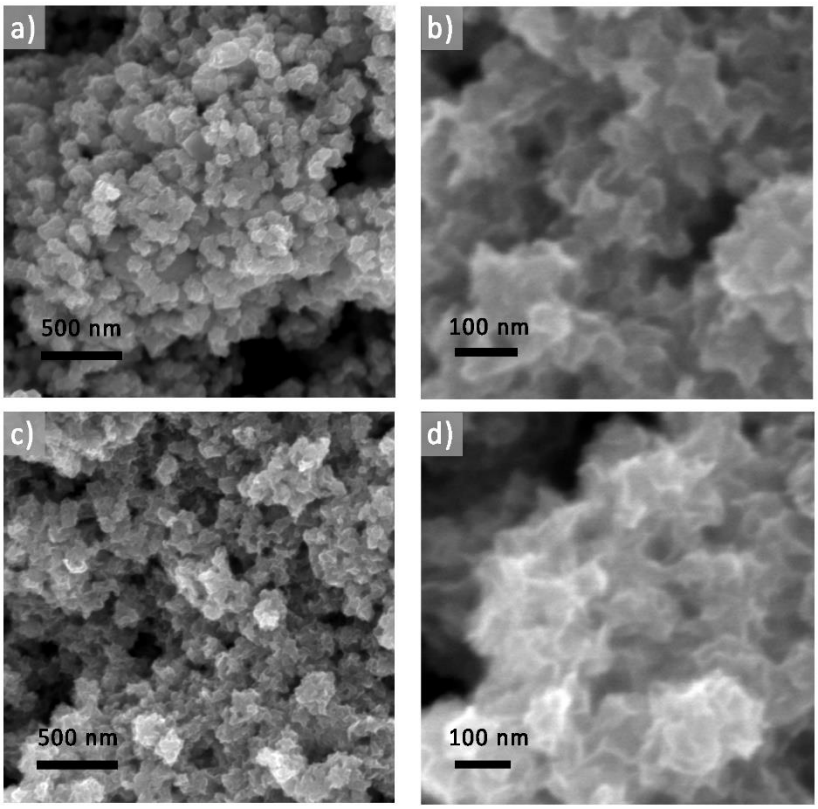

Figure S1. SEM images of (a-b) MoS_2-0HZ and (c-d) MoS_2-1HZ with two scale bars. Similar to MoS_2-4HZ (**Figure** 1a), the macro morphologies of the samples are all uniformly stacked layers of nanosheets.

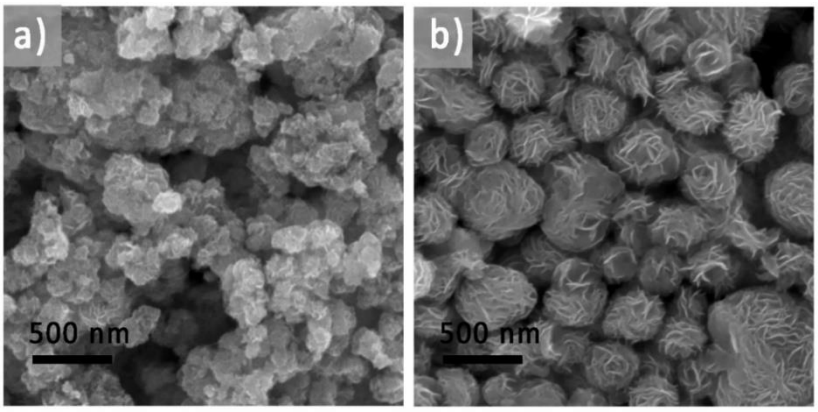

Figure S2. SEM images of a) MoS_2-4HZ-220 and b) MoS_2-0HZ-220. Compared to the three samples we discussed in the manuscript, the change of synthesizing condition refers to higher hydrothermal temperature (220 °C compared to 180 °C). The morphology of MoS_2-4HZ-220 almost maintains the same as MoS_2-4HZ-180, while MoS_2-0HZ-220 exhibits more stacked nano-flowers. The morphology of the MoS_2 synthesized without hydrazine is dependent on temperature.

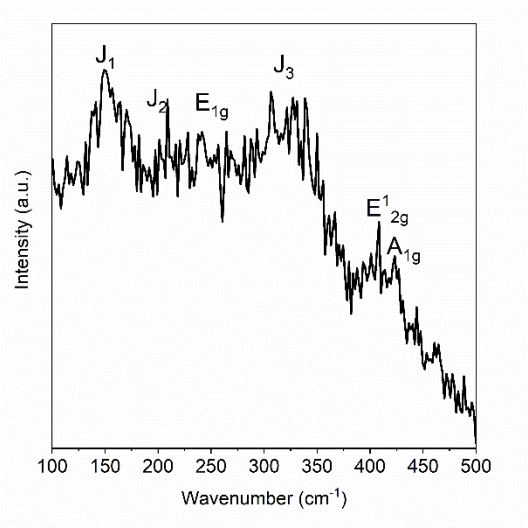

Figure S3. Raman spectra of sample MoS_2-4HZ-220.

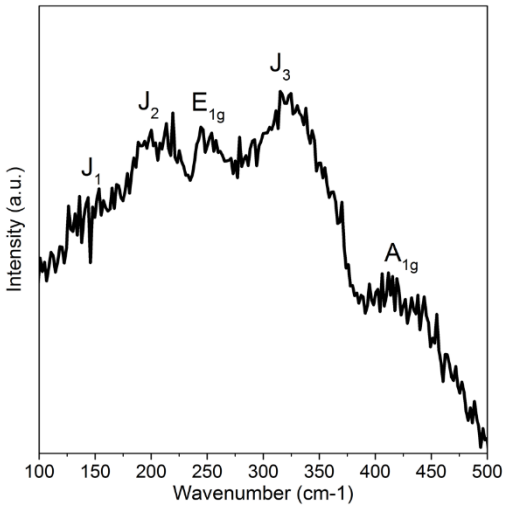

Figure S4. Raman spectra of MoS_2-4HZ powder after being stored at room temperature for 3 months.

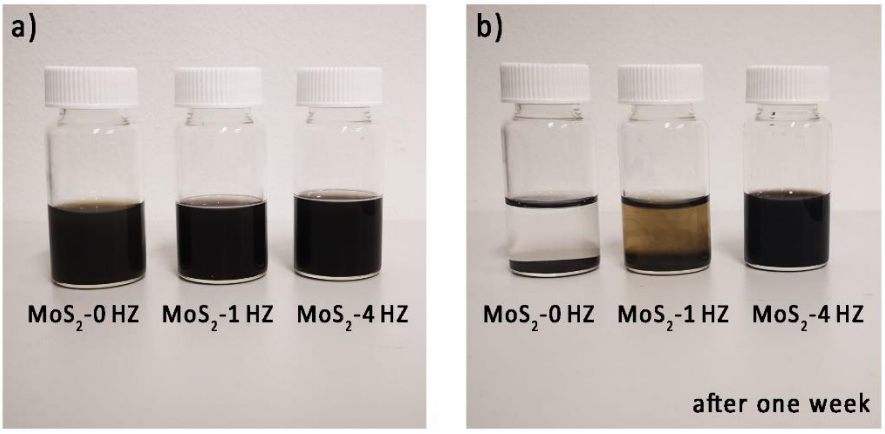

Figure S5. The solutions of sample MoS_2-0HZ, MoS_2-1HZ, and MoS_2-4HZ. Each jar contains a mixture of 15 mg sample powder and 15 mL DI water, and the set is ultrasonicated for 20 min to form a homogeneous solution. The image is taken a) right after the preparation; b) after waiting for 1 week.

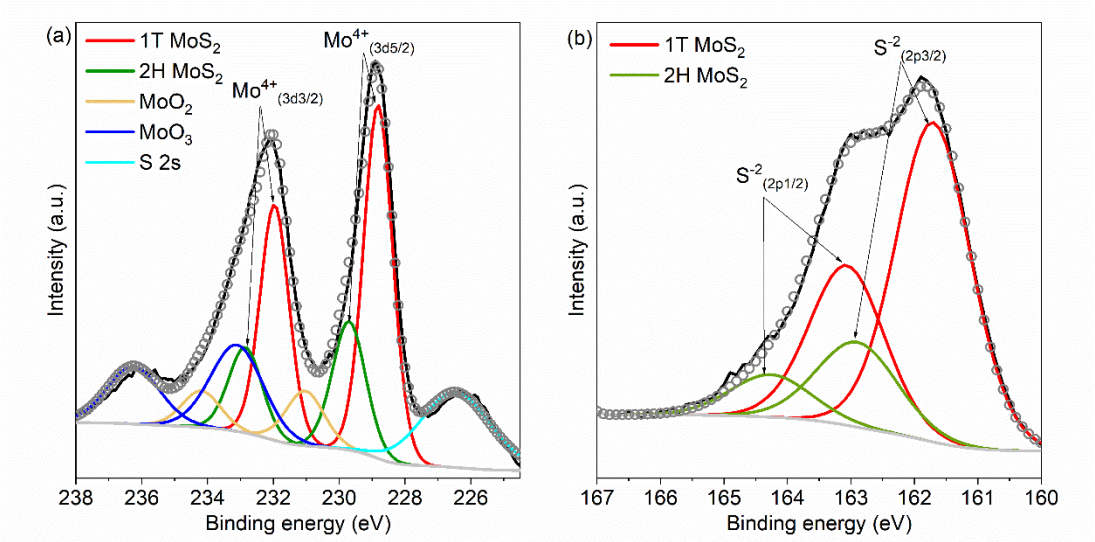

Figure S6. XPS spectra associated with a) Mo (3d) and b) S (2p) of sample MoS_2-4HZ-220. The spectra are very similar to that of MoS_2-4HZ, and the calculated relative 1T phase quantification is ~70% (consistent with ~69% of MoS_2-4HZ), indicating that the higher reaction temperature (220 °C compared to 180 °C) does not have an obvious impact on the percentage of 1T phase.

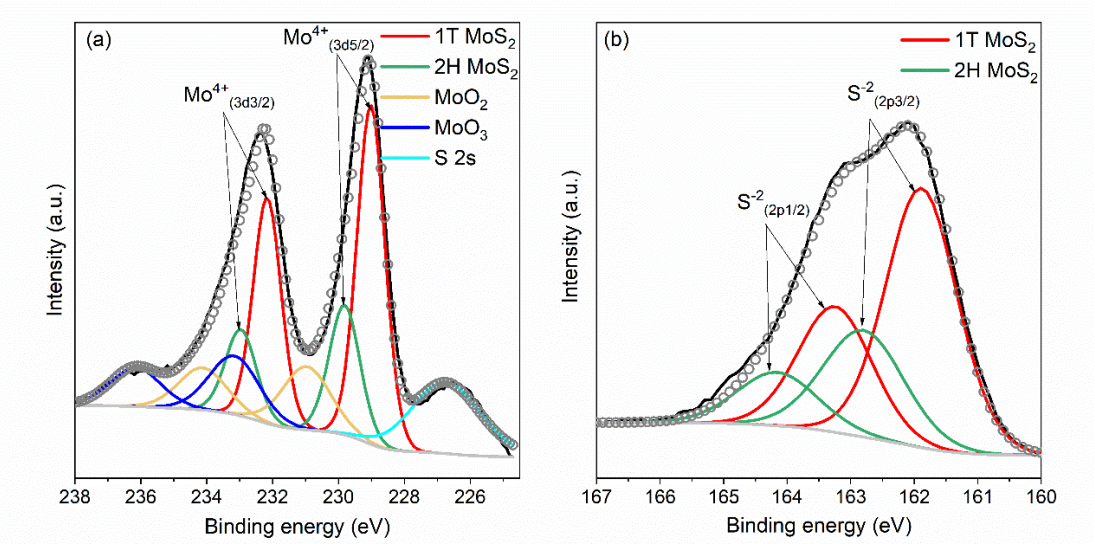

Figure S7. XPS spectra associated with a) Mo (3d) and b) S (2p) of sample MoS_2-12HZ. The spectra are very similar to that of MoS_2-4HZ, and the calculated relative phase quantification (~70% 1T) is consistent with MoS_2-4HZ (~69%), indicating that excess hydrazine does not lead to a higher percentage of 1T phase.

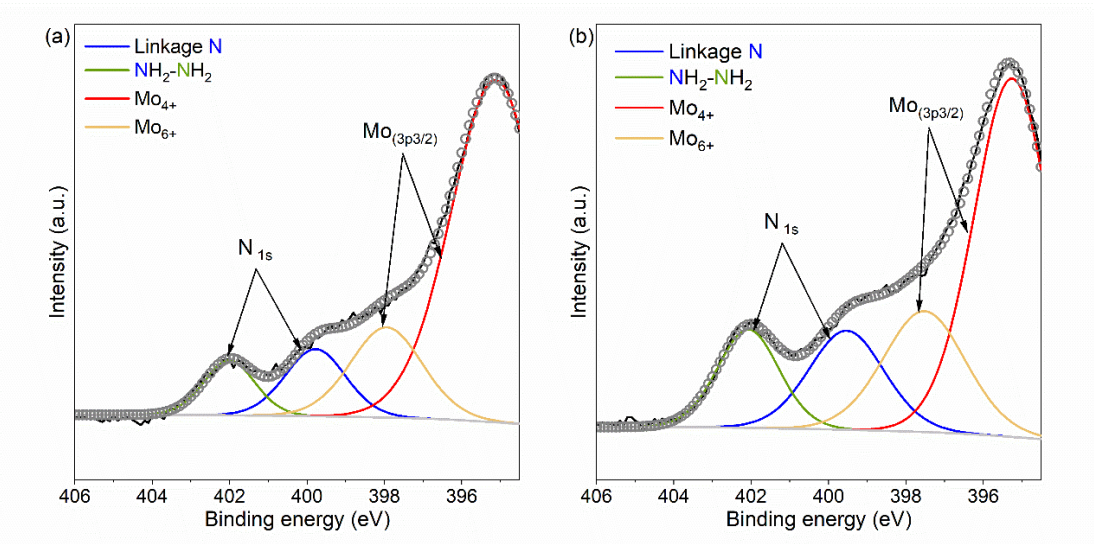

Figure S8. XPS spectra associated with N (1s) of sample (a) MoS_2-1HZ and (b) MoS_2-4HZ.

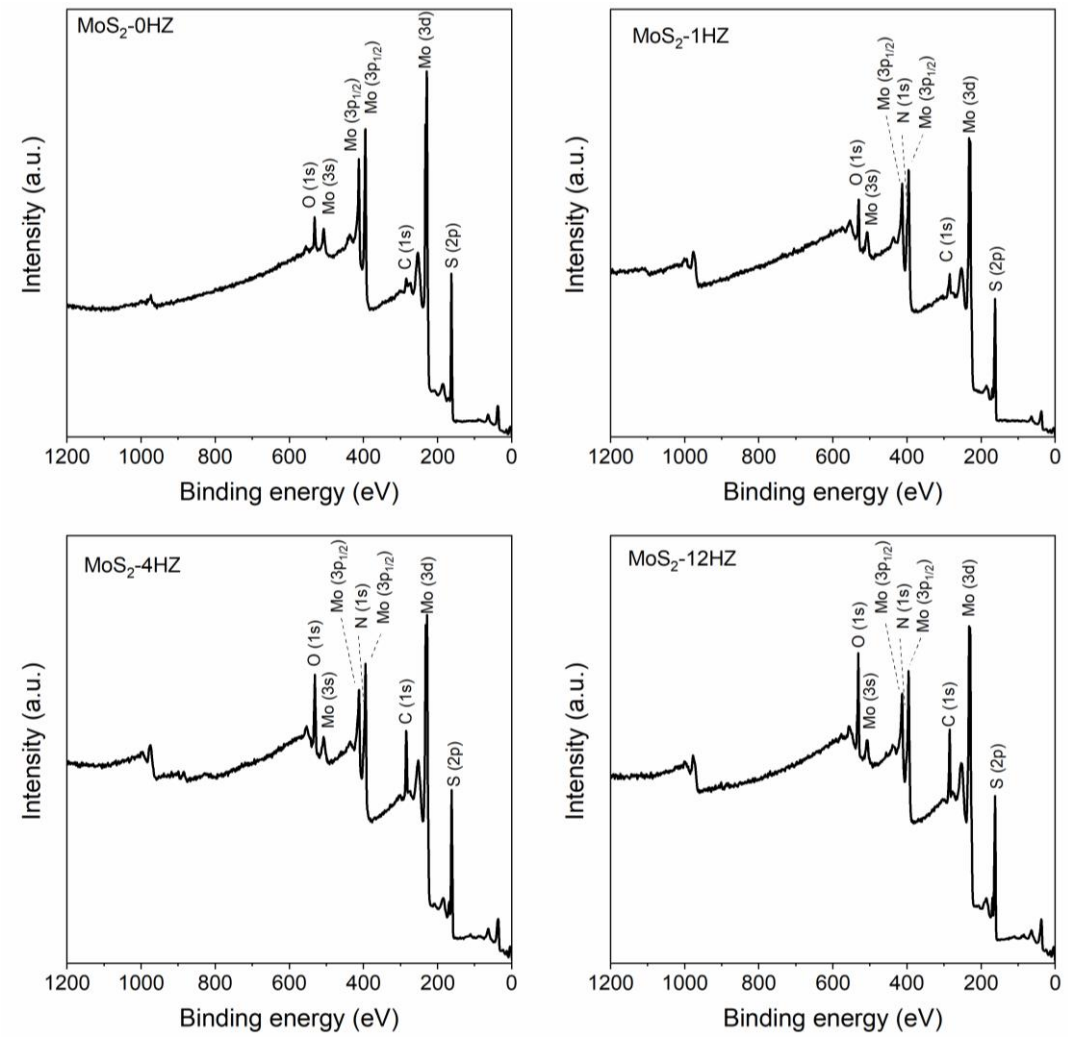

Figure S9. XPS survey scan of sample MoS_2-0HZ, MoS_2-1HZ, MoS_2-4HZ, and MoS_2-12HZ.

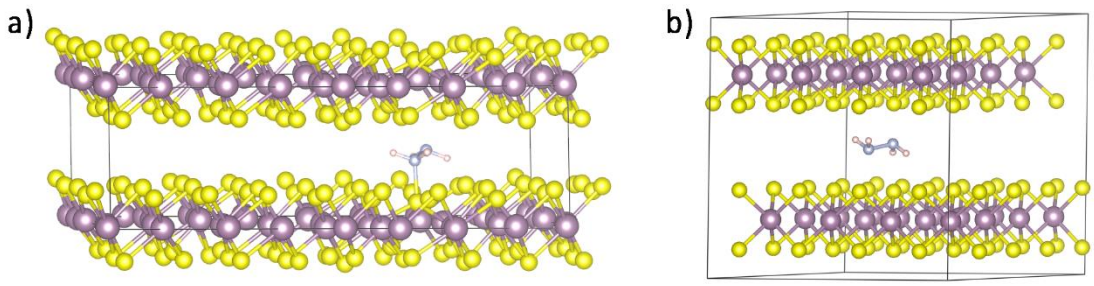

Figure S10. Structure of fully geometry optimized 1T-MoS_2 + N_2H_4 and 2H-MoS_2 + N_2H_4.

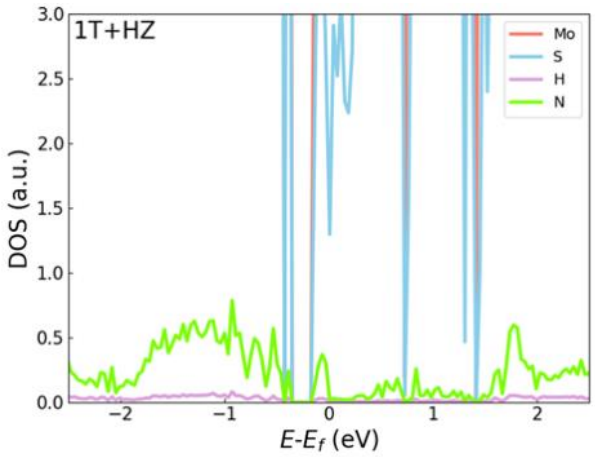

Figure S11. The zoomed-in image of **Figure** 4b, representing the electronic density of state (DOS) for each element of 1T-MoS_2 +HZ.

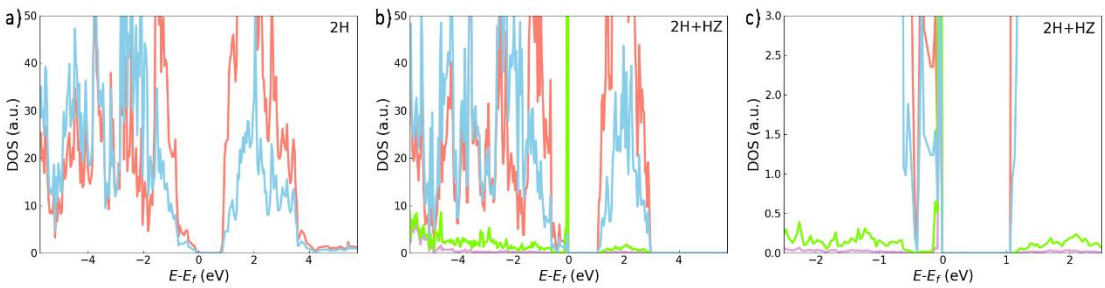

Figure S12. DOS for each element of a) 2H-MoS_2, b) 2H-MoS_2 + HZ, and c) zoomed-in DOS of 2H-MoS_2 +HZ. The DOS of N and H are scaled to a factor of 7.5 for better visualization. The Fermi energy (E_f) has been shifted to zero ($E - E_f = 0$). Mo, S, H, and N partial contributions to the DOS are represented with red, blue, violet, and green lines, respectively.

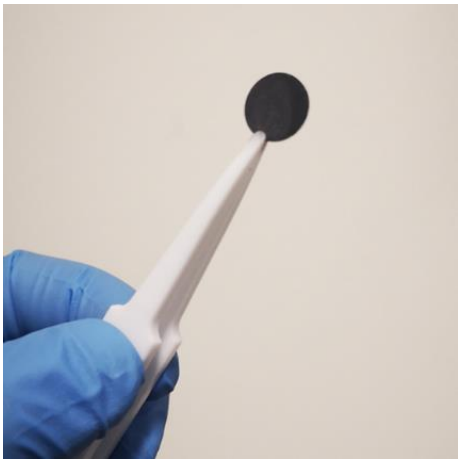

Figure S13. The MoS_2 pellets were compressed by 60 mg powder of each sample and were used to test electrical conductivity with the four-point probe equipment.

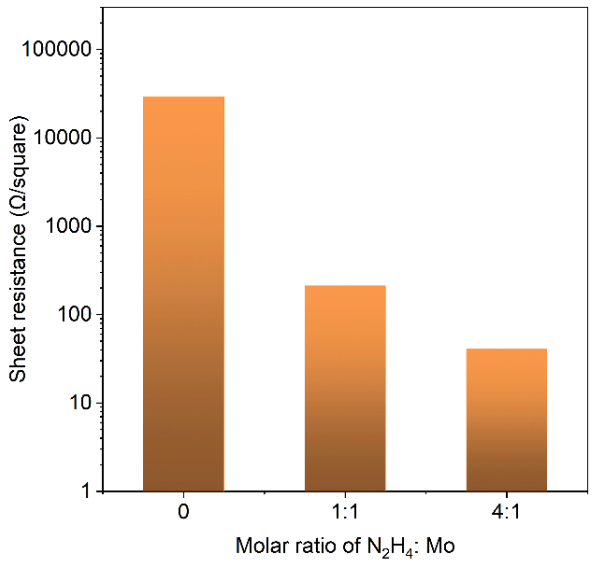

Figure S14. The sheet resistance of sample pellets MoS_2-0HZ, MoS_2-1HZ, and MoS_2-4HZ.

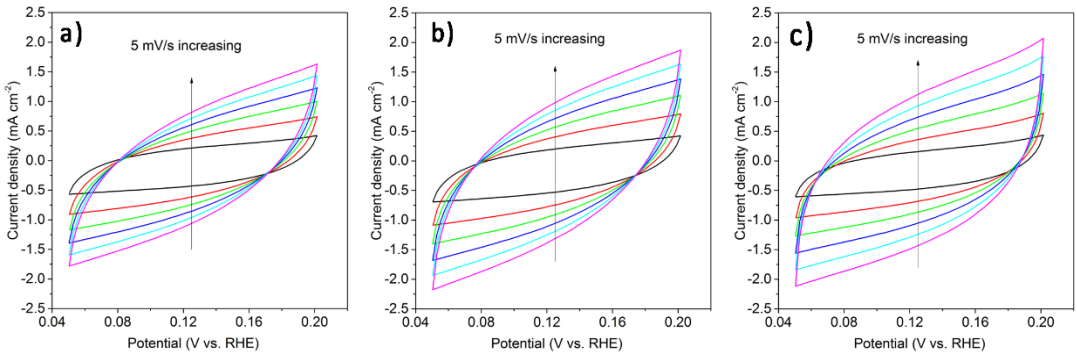

Figure S15. CV curves in the non-faradaic region at scan rates of 5, 10, 15, 20, 25, and 30 mV/s for sample a) MoS_2-0HZ, b) MoS_2-1HZ, and c) MoS_2-4HZ.

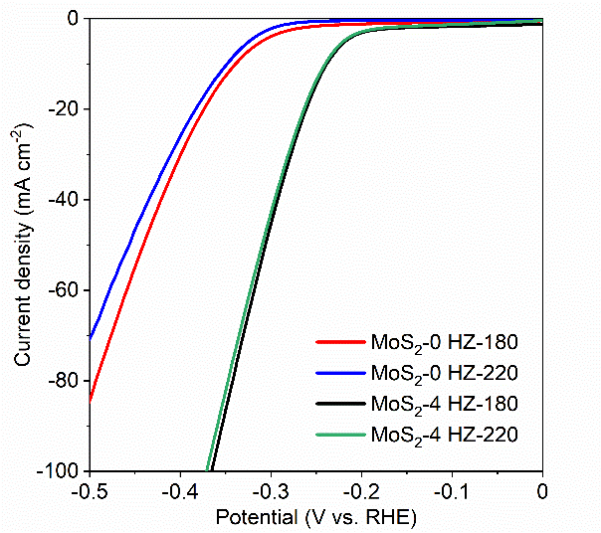

Figure S16. HER LSV polarization curves of sample MoS_2-0HZ and MoS_2-4HZ synthesized at 180°C and 220°C, respectively.

Table S1. The nominal and actual atomic ratio of the samples identified by XPS measurement.

Sample	Mo: S: N molar ratio	1T phase proportion
MoS_2-0HZ	1: 2.2: 0	0%
MoS_2-1HZ	1: 1.9: 0.031	22%
MoS_2-4HZ	1: 2.1: 0.089	69%
MoS_2-12HZ	1: 2.2: 0.125	70%

Table S2. Ground state energy of 1T-MoS_2, 1T-MoS_2 + N_2H_4, 2H-MoS_2, and 2H-MoS_2 + N_2H_4, and intercalation energy of 1T-MoS_2 and 2H-MoS_2.

	1T	2H
E_{MoS2}	-548.91781 eV	-573.25277 eV
$E_{MoS2+N2H4}$	-585.35072 eV	-602.02779 eV
E_{N2H4}	-303.16257 eV	-303.16257 eV
$E_{intercalation}$	-6.116653 eV	1.54124 eV

Table S3. The sheet resistance of sample MoS_2-0HZ, MoS_2-1HZ, and MoS_2-4HZ.

Sample pellet	MoS_2-0HZ	MoS_2-1HZ	MoS_2-4HZ
Sheet resistance (Ω/square)	28,946	211.6	41.1

Table S4. Summary of HER performance. Onset potential is derived from the linear fit of the Tafel slope; Resistance is equal to the radius of the EIS curve; ECSA is calculated from C_{dl}.

Catalysts	Onset potential (mV)	η (mV) at j=10 mA cm^{-2}	Tafel slope (mV dec^{-1})	R_{CT} (Ω)	ECSA (cm^2)
MoS_2-0HZ	286	340	99	246	609.62
MoS_2-1HZ	242	284	74	53.3	787.23
MoS_2-4HZ	196	230	64	30.4	970.66